

INFRARED OBSERVATIONS OF THE MOON AND THEIR INTERPRETATION

M. J. PUGH and J. A. BASTIN

Dept. of Physics, Queen Mary College, University of London, London, England

Abstract. The lunar spectrum, resulting from both the directly scattered solar radiation and the Moon's intrinsic thermal radiation, is described. The variations of the thermal component with latitude and phase, and during eclipse conditions, are described and compared with a plane homogeneous model of temperature-independent thermal constants. A review is given of that data appropriate to the lunar crust which may be obtained, both from comparison of this model with observation and from those modifications of the model, which explain otherwise anomalous measurements. Finally, a discussion of the various methods of determining the vertical temperature gradient at the surface leads to a mean value of about 2K m^{-1} , although the heat flux associated with these results is much less than the recent direct measurement.

In view of the direct measurements of the temperature and thermal gradients of the regolith made very recently, and to be described for the first time at this conference, it is appropriate to consider and review the knowledge of the temperature and thermal properties of the top surface layer of the Moon which may be derived from a study of the Moon's thermal radiation observed by Earth-based telescopes.

1. The Lunar Spectrum

Figure 1 shows a simplified spectrum of lunar radiation which covers the whole range of wavelengths in which the Moon emits measurable amounts of electromagnetic radiation. In general the radiation is a sum of two terms consisting respectively of scattered solar radiation and lunar thermal radiation

$$I_{\lambda} = AB_{\lambda}(T_s) \left(\frac{r_s}{R_m} \right)^2 + (1 - A) B_{\lambda}(T_m). \quad (1)$$

In this expression A is the albedo of the lunar surface; r_s the solar radius; R_m the mean Moon-Sun distance; T_s and T_m the solar and lunar temperatures respectively; and $B_{\lambda}(T)$ is the Planck black-body radiation function at temperature T . In the first term which represents scattered solar radiation we have assumed for simplicity that the Moon is a Lambertian scatterer, an assumption which, while far from true, will not affect our discussion of thermal radiation. The temperature T_s we have taken to be 5600 K, and the lunar temperatures which we have assumed are 400 K during the lunar day, and 100 K during the night.

A closer approximation to reality may be found by allowing T_s and T_m to be wavelength-dependent. T_s is then the solar brightness temperature which will vary in the range 4000–6000 K at wavelengths below about 2×10^{-3} m, rising to some 300 times this value at longer wavelengths. $T_m(\lambda)$ is the brightness temperature of the lunar surface at wavelength λ . At wavelengths below about 300 μm this is essentially the

surface temperature, whereas at longer wavelengths it is a function of temperatures at all depths, weighted by an absorption factor

$$B_{\lambda}(T_m(\lambda)) = \int_{z=0}^{z=\infty} K_{\lambda} Q B_{\lambda}(T_z) e^{-K_{\lambda} \rho z} dz, \quad (2)$$

where z is the distance measured into the lunar crust in the direction from which the

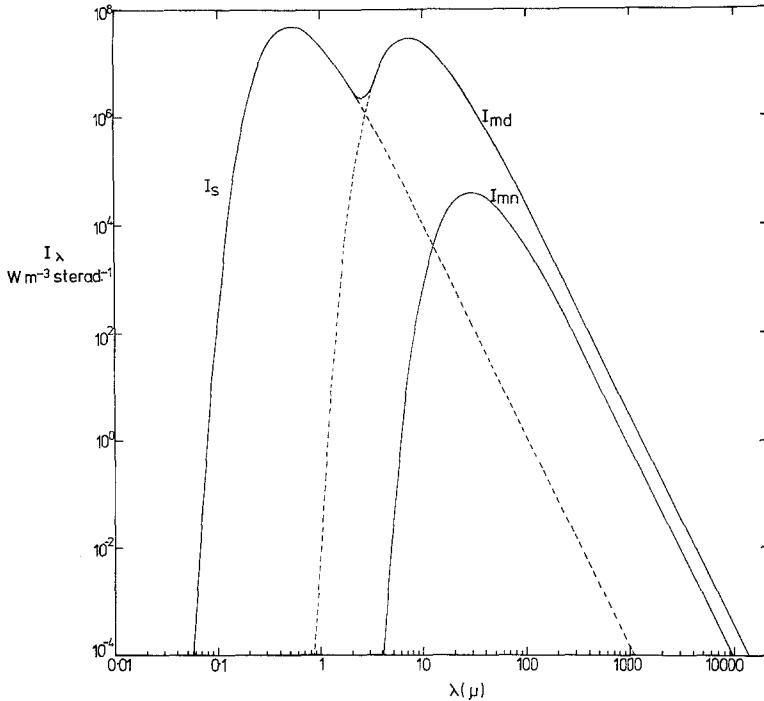


Fig. 1. The lunar electromagnetic spectrum based on a simplified model which assumes the Sun to have a black body spectrum and the lunar albedo and emissivity to be wavelength independent. The continuous curve labelled I_s and I_{ma} is the predicted spectrum at lunar noon on the equator; the right hand peak representing lunar thermal radiation whereas the left hand peak results from directly scattered solar radiation. I_{mn} is the predicted spectrum at lunar midnight on the equator.

outgoing ray emanates. At the centre of the Moon's disc this will simply be the vertical direction.

Figure 1 shows that during the lunar day, lunar thermal radiation dominates scattered solar radiation for all wavelengths above about 4μ . Figure 2 shows approximately the wavelength ranges in which terrestrial atmospheric transmission makes Earth-bound observation possible, and the relevance of the measurements to the determination of various properties of the lunar surface. Although in astronomy we are no longer limited to ground-based observation, it is nevertheless the case that the only useful lunar infrared observations at present available have been made from ground-based sites.

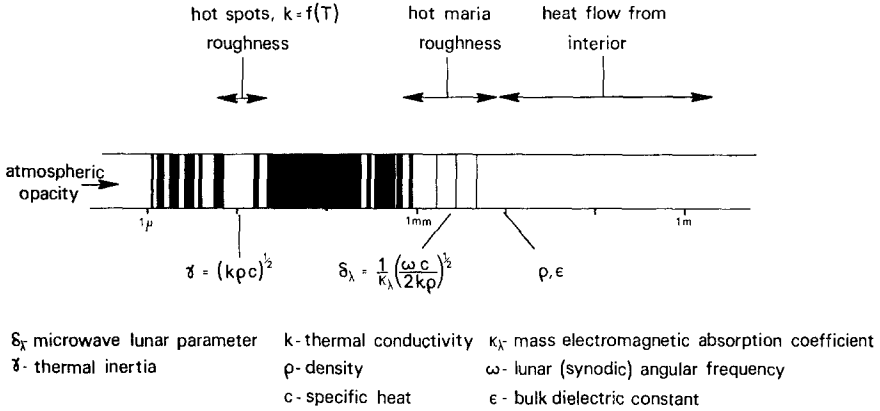


Fig. 2. Observations of the Moon in infrared and radio wavelength regions. The light portions in the spectrum indicate essentially those wavelength regions for which ground based observations are possible. Both above and below the spectrum are indicated the information about the lunar surface which may be obtained from telescopic observations in the various wavelength ranges.

2. The Surface Heat Balance

It is convenient to compare infrared and radio range observations of the Moon's thermal radiation with a simplified theoretical model. Not only may the values of various physical surface parameters be determined as a result of the comparison, but also deviations between observation and the predictions of the model indicate other localized or global properties of the lunar surface. The simplest model to adopt for a study of the surface thermal balance is the plane homogeneous model in which the lunar surface is considered to be flat, horizontal, and composed of material whose thermal characteristics do not vary either spatially or with temperature. Any element of the lunar surface is alternately heated and cooled in a monthly cycle resulting from the rotation of the Moon with respect to the direction of the incoming solar radiation.

Within the surface material the model predicts that the variation of temperature T_z at depth z will obey the one-dimensional diffusion equation for space and time of the form

$$\frac{\partial T_z}{\partial t} = \frac{K}{\rho c} \left(\frac{\partial^2 T_z}{\partial z^2} \right). \tag{3}$$

In this equation t represents the time; K , ρ , and c are the thermal conductivity, density, and specific heat, respectively. The imposed boundary conditions are that the thermal flux at $z = \infty$ is zero, and that at the surface there is a balance between the incoming absorbed solar insolation, and the heat radiated from and conducted into the surface: namely,

$$-K \left(\frac{\partial T_z}{\partial z} \right) = (1 - \alpha_1) I - (1 - \alpha_2) \sigma T_0^4, \quad z = 0 \tag{4}$$

where I is the solar insolation (i.e. the amount of solar energy incident per unit time per unit area on the lunar surface); α_1 is the fraction of this energy which is reflected or scattered directly; σ is Stefan's constant and $(1 - \alpha_2)$ is the emissivity of the surface, averaged over the infrared region in which the Moon emits thermal radiation and weighted at each wavelength in proportion to the intensity of this radiation. The constants α_1 and α_2 may thus be regarded as albedo for incoming and outgoing radiation at the lunar surface. During a normal lunation cycle the insolation is related to

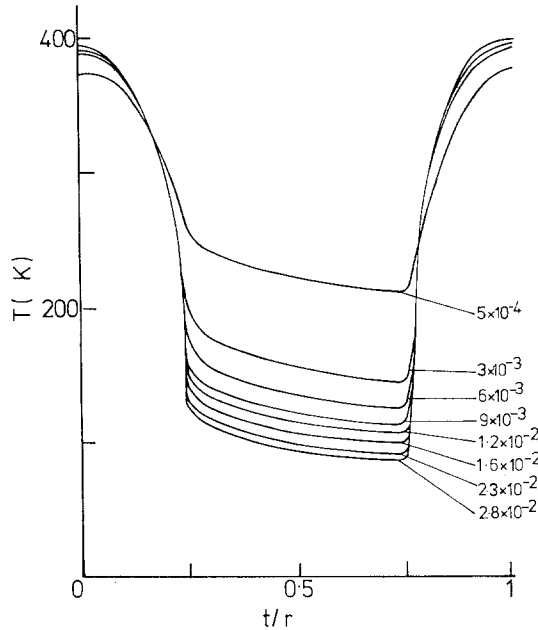


Fig. 3. Temperatures of a point on the lunar equator shown as a function of time during a lunation computed for the plane homogeneous model using various values of the thermal inertia parameter $(K\rho c)^{-1/2}$. The numbers by each curve represent this parameter in units $\text{km}^2 \text{s}^{+1/2} \text{J}^{-1}$ (From Troitski, 1967; $1 \text{K cm}^2 \text{s}^{+1/2} \text{cal}^{-1} = 2.39 \times 10^{-5} \text{km}^2 \text{s}^{+1/2} \text{J}^{-1}$).

the solar constant f and the solar zenith angle ξ :

$$I = f \cos \xi, \quad 0 < \xi < \pi/2 \text{ (lunar day);} \tag{5}$$

$$I = 0, \quad \pi > \xi > \pi/2 \text{ (lunar night);} \tag{6}$$

while during an eclipse the insolation drops to a value of β times that given in Equation (5), where β is less than unity and is zero during totality.

The solutions of Equations (3)–(6) require the use of medium-sized computers and there exists a considerable amount of literature describing the work (Jaeger, 1953 (a) and (b); Krotikov and Shchuko, 1963; Bastin and Gough, 1969). For a given surface albedo the results of the computation are a function of the single variable $K\rho c$, usually represented by a quantity known as the thermal inertia $\gamma = (K\rho c)^{-1/2}$.

Computed surface temperatures for different values of this parameter are shown in Figure 3.

A comparison between the theoretical predictions shown in Figure 3 and infrared determinations of the brightness temperature indicate a very low value for the conductivity. Since, as is seen from this figure, the daytime temperature is only weakly dependent on the conductivity, the determination of the value of $(K\rho c)^{-1/2}$ to be adopted depends essentially on measurements of the lunar surface temperature during eclipse and during the lunar night. We shall later discuss the finer points of the comparison between theory and experiment in these two cases: however, within a factor

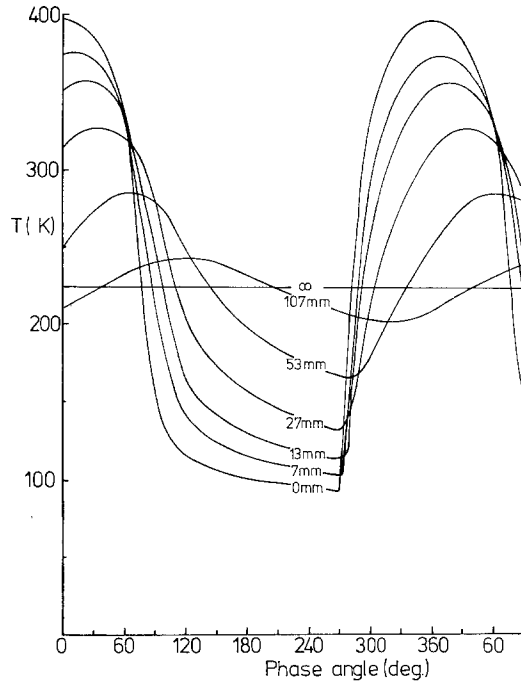


Fig. 4. Surface and subsurface temperatures at the lunar equator computed as a function of lunar phase. The numbers by the individual curves refer to the depths below the surface. A value of $(K\rho c)^{-1/2} = 2.3 \times 10^{-2} \text{ km}^2 \text{ s}^{+1/2} \text{ J}^{-1}$ has been assumed.

of about 2, both methods agree in assigning a value of $(K\rho c)^{-1/2} = 2.4 \times 10^{-2} \text{ m}^2 \text{ s}^{1/2} \text{ KJ}^{-1}$ to the top lunar surface layer. Figures 4 and 5 show computations of the surface and subsurface temperatures during a lutation and during eclipse, using this value for $(K\rho c)^{-1/2}$. It is seen that the lutation temperature wave is damped to $1/e$ of its surface amplitude within about 80 mm of the surface. In the eclipse case the penetration of the thermal effect is reduced by about 10 in distance.

The measured form of the variation of surface temperature throughout a normal lutation and during eclipse conditions agree to a good approximation with that

predicted by theory. Exact comparison, however, shows a number of discrepancies, a study of which is useful in indicating the nature of the lunar surface layer. The discrepancies or anomalies have been listed (e.g. by Bastin and Gough, 1969). We may usefully define such an anomaly as any effect not expected on the basis of the plane homogeneous model: they may be classified in terms of the explanations which account for them:

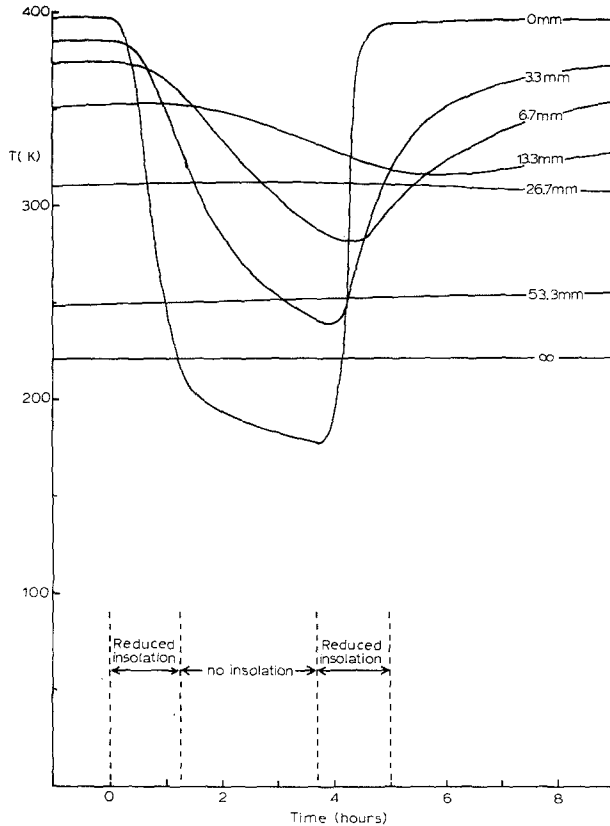


Fig. 5. Computed surface and subsurface temperatures at points on the lunar equator, during an eclipse of the Moon. The numbers by the individual curves refer, in each case, to the depth below the surface. A value of $(K\rho c)^{-1/2} = 2.3 \times 10^{-2} \text{ km}^2 \text{ s}^{+1/2} \text{ J}^{-1}$ has been assumed (from unpublished calculations by D. O. Gough).

- (i) Variation of the thermal properties with depth.
- (ii) Changes of the thermal properties of the regolith over the lunar surface.
- (iii) Variation of the thermal properties with temperature.
- (iv) The effects of surface roughness.

All the discrepancies between observation and the predictions of the plane homogeneous model have been accounted for in terms of one or more of the above effects.

3. Variations of Thermal Properties of the Regolith with Depth and Temperature

The plane homogeneous model cannot account for the very slow variation of measured brightness temperature in the infrared (8–14 μm) during the umbral stages of an eclipse. Jaeger and Harper (1950) analyzed eclipse measurements of lunar temperatures and showed that a model with a fine layer of low conductivity material overlying a more thermally conductive substratum, is in better agreement with observations than

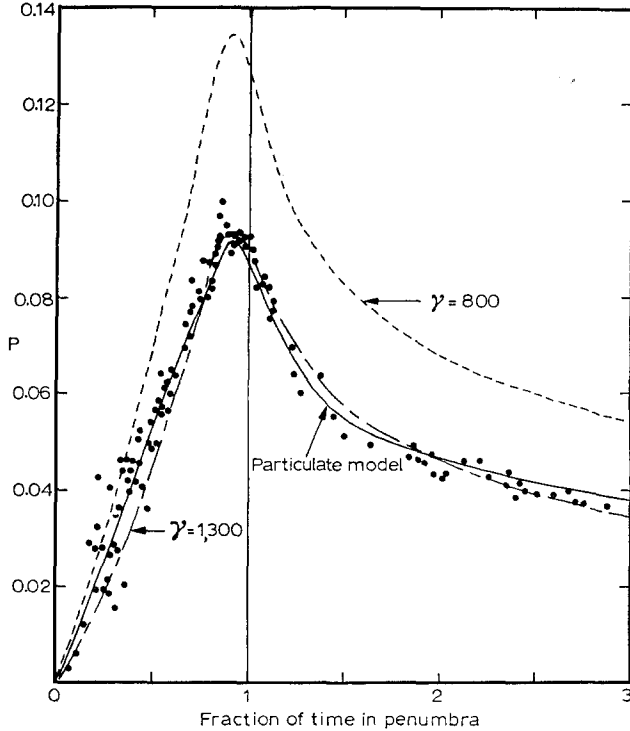


Fig. 6. Measurements made of lunar radiation in the 8–14 μm wavelength range during an eclipse (filled circles together with the predictions (continuous curve), for the centre of the lunar disc, of the *Particulate Thermophysical Model* of Winter and Saari (1969). The quantity P is a 'differential energy parameter' defined by these authors. It is clear that the particulate model, which assumes increases of conductivity with depth and temperature, gives better agreement with observation than any of the smooth homogeneous model.

any plane homogeneous model. More recently Winter (1970) has confirmed the same general effect by considering a model in which the conductivity increases continuously with depth (see Figure 6). Piddington and Minnett (1949) came to the same conclusion as a result of analyzing millimetre wavelength brightness temperature measurements throughout a lunation. These measurements essentially refer to deeper layers (0–100 mm) than do the eclipse measurements (0–10 mm). There still seems some doubt about the magnitude of the lowering of the millimetre brightness temperatures during eclipses

(Baldock *et al.*, 1965; Low, 1965; Gibson, 1961). However, since it is now accepted that the conductivity of the immediate top layers of the lunar surface is probably considerably lower than had been anticipated from earlier analyses, it now seems likely that all the millimetre eclipse data are consistent with some increase of thermal conductivity with depth. A variation of conductivity with depth is also implied by laboratory far infrared measurements of lunar rock (Bastin *et al.*, 1970; Ade *et al.*, 1971) which show for the top few centimeters of the surface a much lower conductivity than that measured directly at greater depths (~ 1 m) by the lunar heat flux experiment and reported at this conference (Langseth, 1971). Since it is known that interparticle contacts affect the conductivity it is possible that gaseous adhesion at these greater depths increases the conductivity. The gaseous pressure required for such adhesion is probably about 10^{-5} mb. Other more obvious possibilities are, of course, that the particle contacts are increased by pressure with depth, or that the actual gaseous pressure becomes sufficient to cause an appreciable contribution to the conductivity (10^{-3} mb).

The variation of thermal properties with temperature may be attributed to at least three effects each of which gives rise to an effective decrease of the parameter $(K\rho c)^{-1/2}$ with temperature.

A. A RADIATIVE COMPONENT IN THE HEAT TRANSFER

It may be shown that thermal transfer by radiation gives rise to a term which formally appears as a conduction term and varies in magnitude as T^3 . The subject has been considered by (Wesselink, 1948; Kopal, 1964; Clegg *et al.*, 1965; Linsky, 1965 and Winter, 1966). Wesselink (1948) used a simplified model, in comparison with lunar infrared observations to deduce a mean size for the regolith particles. It has since been realized, however, that Wesselink's treatment assumed that the particles were opaque to thermal radiation. Direct analysis of the infrared properties of lunar rock (Bastin *et al.*, 1970) has shown that an appreciable contribution to the conductivity may occur by radiation transfer through the regolith particles so that Wesselink's result was more in the nature of an estimate of the mean path length for infrared photons.

B. VARIATION OF THE LATTICE CONDUCTIVITY WITH TEMPERATURE

The lattice theory of solids predicts a thermal conductivity which drops to zero at the absolute zero of temperature. This prediction is in agreement with measurements so far made with samples of lunar rocks and breccia. (Horai *et al.*, 1970; Warren *et al.*, 1971.) In the case of the crystalline rock, values of the conductivity in the temperature range 200–400 K are in the range $1-1.5 \text{ Jm}^{-1} \text{ s}^{-1} \text{ K}^{-1}$, dropping to values in the range $1-10 \times 10^{-3} \text{ Jm}^{-1} \text{ s}^{-1} \text{ K}^{-1}$ at around 4 K. The breccia has conductivity 3 times lower at room temperature and as much as 10 – 100 times lower in the lower range.

C. A DECREASE OF SPECIFIC HEAT OF CRYSTALLINE AND GLASSY MATERIALS WITH DECREASING TEMPERATURE

This effect has been confirmed in the case of lunar fines and other rock-types by Robie *et al.* (1971).

The combined effect of these three temperature dependencies indicates a rapid variation of the effective conductivity and of the parameter $(K\rho c)^{-1/2}$ with temperature. Two results of this temperature dependence have been observed in the study of lunar thermal radiation:

(a) The drop of temperature during the first stage of eclipse cooling is not so rapid as that predicted on the basis of the plane homogeneous model. (Jaeger and Harper, 1950; Winter and Saari, 1970; Clegg *et al.*, 1965.)

(b) When averaged over the lunar cycle the mean millimetre brightness temperature is considerably higher than the mean infrared (8–14 μm) temperature which essentially relates to surface temperatures. The millimetre brightness temperatures relate to subsurface conditions and on the basis of a temperature-dependent conductivity these would be expected to be higher than the mean surface temperature since the top lunar layer acts essentially as a rectifier during the lunar cycle (Muncey, 1958, 1963; Clegg *et al.*, 1965; Linsky, 1966).

4. The Effects of Surface Roughness

The advent of high speed computers has made possible the solution of the heat balance problem in cases where the surface is composed of a more or less complex profile. In particular, the following models have been discussed:

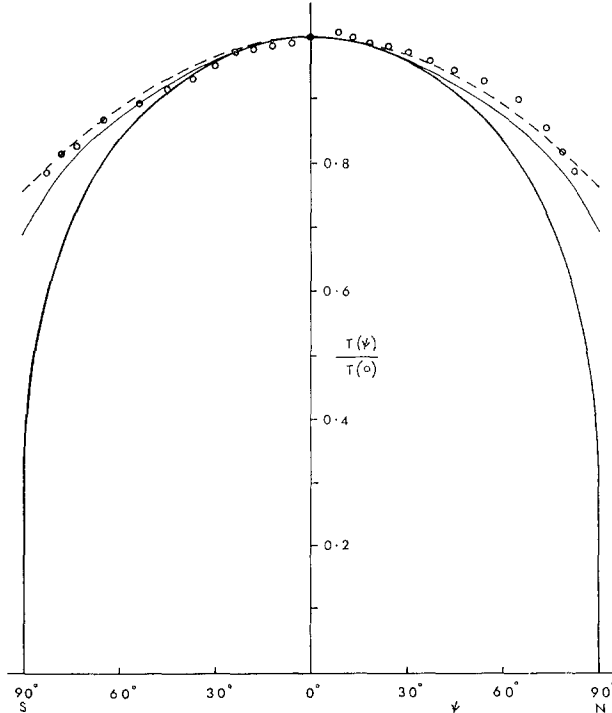


Fig. 7a.

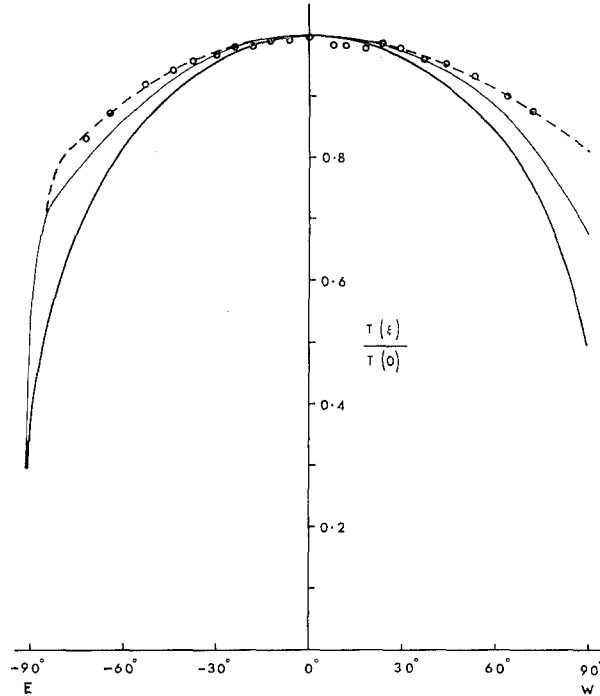


Fig. 7b.

Figs. 7a-b. (a) Poleward variation of the meridian brightness temperature measured at full Moon and at a wavelength of $11 \mu\text{m}$; (b) Equatorial brightness temperatures measured at $11 \mu\text{m}$ wavelength at full Moon. In both diagrams the open circles refer to the measurements of Saari and Shorthill, 1967. The thick continuous curve indicates the predictions of the plane homogeneous model. The thin continuous curve is for a trough model in which the trough depth, width, and the width of the raised portions are all 0.04 m. The broken curve is the same except that the width of the troughs is in this case 0.12 m.

- (i) Hemispherical craters (Buhl *et al.*, 1968(a) and (b))
- (ii) An indented trough model (Bastin and Gough, 1969).
- (iii) A model with surface rocks (Roelof, 1968).

These calculations explain a number of global effects including the apparently high brightness temperatures of the lunar limbs at full Moon (Figure 7) and the variation of the apparent brightness temperature of the subsolar point with the direction of observation. The model proposed by Roelof is not only dependent on the aspect and shadowing effects of the rocks but also assumes conductivities for these rocks appropriate to basaltic samples and in this respect his model is a composite of a rough model and those to be described in the next section.

5. Localized Variations in the Thermal Properties of the Regolith

It now seems virtually certain that the hot spots discovered by Saari and Shorthill

(1965) are the result of localized regions of higher thermal conductivity than the surroundings. The alternate roughness explanation (Bastin, 1965) is not tenable, since the hot spot regions are not found to remain hotter during the lunar day. Not only do the hot spots coincide with regions in which we might expect a preferentially large amount of small size rocks lying on the surface but multiband photometry in the range 2–20 μm both during eclipses and the lunar night can only satisfactorily be explained

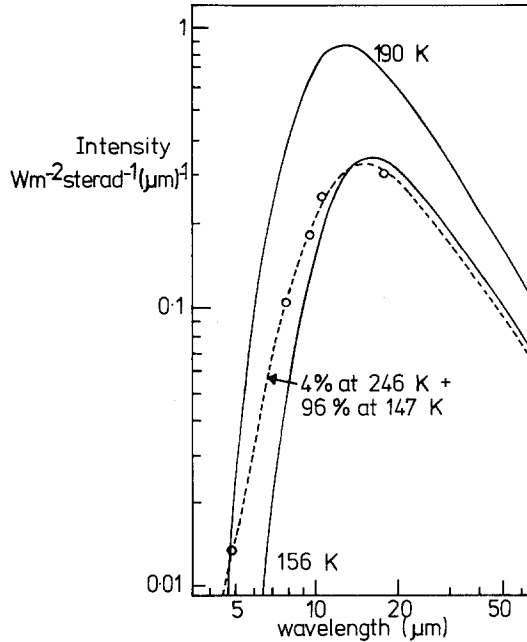


Fig. 8. Multicolour photometry of the south polar region of the Moon during the partial eclipse of Feb. 1970. Open circles show measurements by Allen (Allen and Ney, 1969). The two Planck curves marked 156K and 190K do not give good agreement with observation and it is clear that no single Planck function agrees with the observations. However, the figure shows that a composite surface 4% of which is covered by relatively high temperature material (surface rocks) fits the observations well.

in terms of a composite surface of low conductivity on which are scattered rocks of various sizes but of much higher conductivity (Allen and Ney, 1969; Allen, 1971; see Figure 8).

The presence of such rocks will clearly greatly affect any brightness temperature measurement especially if it is made in the Wien wavelength region in which the intensity varies very rapidly with temperature. It is for this reason that mean surface temperatures should always be measured at as long a wavelength as possible. Thus for example Low (1965) working at 20 μm has obtained a value of 90 K for the mean nighttime lunar equatorial temperature. This is considerably lower than previous measurements at shorter wavelengths (Sinton, 1962; Shorthill and Saari, 1965) yet the

two results may be reconciled by assuming a composite surface of materials at different temperatures. Figure 9 shows the variation of the effective inertial parameter $(K\rho c)^{-1/2}$ which would be expected from different values of the minimum nighttime temperature.

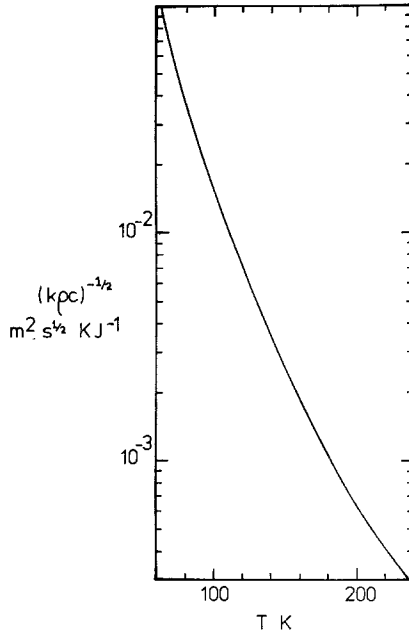


Fig. 9. Thermal inertia $(K\rho c)^{-1/2}$ deduced on the basis of the plane homogeneous model as a function of the lunar surface equatorial temperature just before lunar dawn.

6. The Internal Temperature Gradient

The diurnal thermal wave has an e-folding distance of a few centimetres so that at depths of half a metre or more its effect is negligible and the variation of temperature with depth is that imposed on the regolith layer by the outward heat flux. The thermal gradient at these depths has only recently been determined, and not reported in detail until this conference (Langseth, 1972). However, it is interesting and appropriate to review the other ways in which this gradient has been estimated by less direct means.

(i) The Variation of Lunar Brightness Temperature with Wavelength:

Measurements reported by Troitskii (1967) in the wavelength range 0.1–0.5 m are shown in Figure 10. Throughout the wavelength range the absorption coefficient k_λ of basaltic rocks and glasses is known to vary with wavelength according to the approximate form

$$\rho k_\lambda = A\lambda^{-1}$$

where A is a dimensionless constant (Troitskii, 1967). From direct measurements on

terrestrial basalts and also an extrapolation of measurements on lunar samples at shorter wavelengths (Ade *et al.*, 1971) it is found that the value of A is about 0.05. These measurements together with the results reported by Troitskii indicate a thermal gradient of about 2.5 K m^{-1} . It is important to note that because of the thermal rectifying effect of the top layers we should expect a sharp rise with depth of the mean temperature average throughout a lunation in the top few centimetres of lunar soil; it is, therefore, necessary to consider only those radio measurements in which the diurnal wave has decreased in intensity to a minimal value. It should also be noted

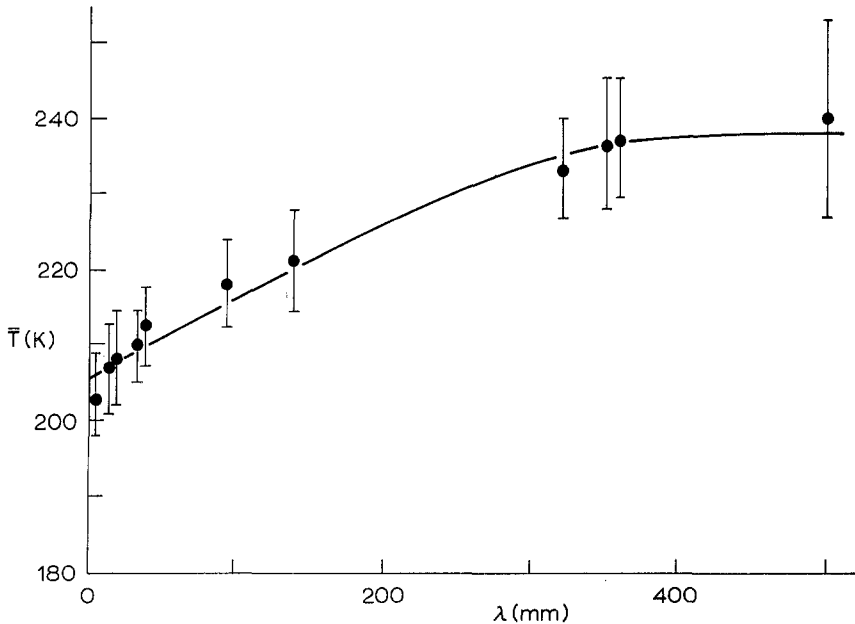


Fig. 10. Brightness temperature averaged over the whole lunar disc and throughout a lunar cycle, shown as a function of the wavelength of observation (Troitskii 1967: a somewhat lower value of the temperature at low wavelengths is indicated by Baldwin, 1961).

that measurements by Baldwin, (1961) show a reduced temperature gradient at greater depths while Salisbury (1971) deduced a negative gradient. It seems that the latter result may be caused by problems in accurate assessment of the beam-width of the telescope used.

(ii) Thermoluminescence of Core-tube Samples:

Hoyt *et al.*, (1971) have claimed that the decrease with depth in the thermoluminescent glow curves of samples taken from the core tubes of Apollo 11 and 12, indicates an internal thermal gradient. The method suffers from the effects of leaky traps (Garlick *et al.*, 1971) and decrease in the intensity of cosmic ionization with depth, but gives a value of $2 \pm 2 \text{ K m}^{-1}$.

(iii) The measurements of Sonett *et al.*, 1971, of the temperature gradient at consid-

erable depths within the Moon (up to 800 km) may be used to determine the thermal gradient in the regolith layer, if the conductivities of the regolith and substratum are known. Thus if K_r and K_s refer to the conductivities of the respective strata, and $(\partial\theta/\partial z)_r$ and $(\partial\theta/\partial z)_s$ to the thermal gradients, then for distances sufficiently small for a steady-state regime to be appropriate (100 km or less) the heat flux Q will be invariant so that:

$$Q = K_r \left(\frac{\partial\theta}{\partial z} \right)_r = K_s \left(\frac{\partial\theta}{\partial z} \right)_s \quad (7)$$

The main uncertainty is in the thermal conductivity of the lunar regolith layer, but if a value $2 \times 10^{-3} \text{ W m}^{-1} \text{ K}^{-1}$ is adopted (Cremers *et al.*, 1970) together with the known values for basaltic rock for K_s ($1-1.5 \text{ W m}^{-1} \text{ K}^{-1}$), then a thermal gradient of about 2 K m^{-1} is deduced. It should be noted, however, that the heat flux deduced in this way is an order of magnitude less than that reported in this conference by Langseth.

References

- Ade, P. A., Bastin, J. A., Marston, A. C., Pandya, S. J., and Puplett, E.: 1971, *Geochim. Cosmochim. Acta, Suppl.* 2, 3, 2203-2211.
- Allen, D. A.: 1971, *The Moon* 2, 435-462.
- Allen, D. A. and Ney, E. P.: 1969, *Science* 164, 419-421.
- Baldock, R. V., Bastin, J. A., Clegg, P. E., Emery, R., Gaitskell, J. N., and Gear, A. E.: 1965, *Astrophys. J.* 141, 1289-1293.
- Baldwin, J. E.: 1961, *Monthly Notices Roy. Astron. Soc.* 122, 513-522.
- Bastin, J. A.: 1965, *Nature* 207, 1381.
- Bastin, J. A. and Gough, D. O.: 1969, *Icarus* 11, 289-319.
- Bastin, J. A., Clegg, P. E., and Fielder, G.: 1970, *Geochim. Cosmochim. Acta, Suppl.* 1, 3, 1987-1991.
- Buhl, D., Welch, W. J., and Rea, D. G.: 1968a, *J. Geophys. Res.* 73, 5281-5295.
- Buhl, D., Welch, W. J., and Rea, D. G.: 1968b, *J. Geophys. Res.* 73, 7593-7608.
- Clegg, P. E., Bastin, J. A., and Gear, A. E.: 1966, *Monthly Notices Roy. Astron. Soc.* 133, 63-66.
- Cremers, C. J., Birkebak, R. C., and Dawson, J. P.: 1970, *Geochim. Cosmochim. Acta, Suppl.* 1, 3, 2045-2050.
- Garlick, G. F. J., Lamb, W. E., Steigmann, G. A., and Geake, J. E.: 1971, *Geochim. Cosmochim. Acta, Suppl.* 2, 3, 2277-2283.
- Gibson, J. E.: 1961, *Astrophys. J.* 133, 1072-1080.
- Horai, K., Simmons, G., Kanamori, H., and Wones, D.: 1970, *Geochim. Cosmochim. Acta, Suppl.* 1, 3, 2243-2249.
- Hoyt, H. P., Miyajima, M., Walker, R. M., Zimmerman, D. W., Zimmerman, J., Britton, D., and Kardos, J. L.: 1971, *Geochim. Cosmochim. Acta, Suppl.* 2, 3, 2245-2263.
- Jaeger, J. C.: 1953a, *Proc. Camb. Phil. Soc.* 49, 355-359.
- Jaeger, J. C.: 1953b, *Austral. J. Phys.* 6, 10-21.
- Jaeger, J. C., and Harper, A. F. A.: 1950, *Nature* 166, 1026.
- Kopal, Z.: 1964, *Icarus* 3, 3-44.
- Krotikov, V. D. and Shchuko, O. B.: 1963, *Sov. Astron. - A.J.* 7, 228-232.
- Langseth, Jr., Marcus G., Clark, Jr., Sydney P., Chute, Jr., John L., and Wechsler, Alfred E., 1972, *The Moon* 4, 390.
- Linsky, J. L.: 1966, *Icarus* 5, 606-634.
- Low, F. J.: 1965, *Astrophys. J.* 142, 806-808.
- Muncey, R. W.: 1958, *Nature* 181, 1458-1459.
- Muncey, R. W.: 1963, *Aust. J. Phys.* 16, 24-31.
- Robie, R. A., Hemingway, B. S., and Wilson, W. H.: 1970, *Geochim. Cosmochim. Acta, Suppl.* 1, 3, 2361-2367.

- Robie, R. A., and Hemingway, B. S.: 1971, *Geochim. Cosmochim. Acta, Suppl.* 2, 3, 2361–2365.
- Roelof, E. C.: 1968, *Icarus* 8, 138–159.
- Saari, J. M. and Shorthill, R. W.: 1965, *Nature* 205, 964–965.
- Salisbury, J. W.: 1971, Private communication.
- Sinton, W. M.: 1962, in *Physics and Astronomy of the Moon* (ed. by Z. Kopal), Chapter 11, Academic Press, New York.
- Sonett, C. P., Colburn, D. S., Dyal, P., Parkin, C. D., Smith, B. F., Schubert, G., and Schwartz, K.: 1971, *Nature* 230, 359.
- Troitskii, V. S.: 1967, *Proc. Roy. Soc. (London)* A296, 366–398.
- Warren, N., Schreiber, E., Scholz, C., Morrison, J. A., Norton, P. R., Kumazawa, M., and Anderson, O. L.: 1971, *Geochim. Cosmochim. Acta, Suppl.* 2, 3, 2345–2360.
- Wesselink, A. J.: 1948, *Bull. Astron. Inst. Netherlands* 10, 351–363.
- Winter, D. F.: 1965, Boeing Document D1-82-0449; also *Int. J. Heat Mass Transfer* 9, 527–532.
- Winter, D. F.: 1967, *Icarus* 6, 229–325.
- Winter, D. F. and Saari, J. M.: 1969, *Astrophys. J.* 156, 1135–1151.